Excited State Intramolecular Proton Transfer and Charge Transfer Dynamics of a 2-(2′-Hydroxyphenyl)benzoxazole Derivative in Solution

Chul Hoon Kim,*,† Jaehun Park,‡ Jangwon Seo,§ Soo Young Park,§ and Taiha Joo*,†

Department of Chemistry, Pohang University of Science and Technology, Pohang, 790-784, Korea, Pohang Accelerator Laboratory, Pohang University of Science and Technology, Pohang, 790-784, Korea, and Center for Supramolecular Optoelectronic Materials and Department of Materials Science and Engineering, Seoul National University, Seoul, 151-744, Korea

Received: October 1, 2009; Revised Manuscript Received: March 29, 2010

Excited state intramolecular proton transfer (ESIPT) and subsequent intramolecular charge transfer (ICT) dynamics of a 2-(2′-hydroxyphenyl)benzoxazole derivative conjugated with an electron withdrawing group (HBOCE) in solutions and a polymer film has been investigated by femtosecond time-resolved fluorescence (TRF) and TRF spectra measurements without the conventional spectral reconstruction method. TRF with high enough resolution (<100 fs) reveals that the ESIPT dynamics of HBOCE in liquids proceeds by at least two time constants of ∼250 fs and ∼1.2 ps. The relative amplitude of the slower picosecond component is smaller in the polymer film than that in solution. Conformational heterogeneity in the ground state originating from the dispersion of the dihedral angle between the phenolic and benzoxazole groups is invoked to account for the dispersive ESIPT dynamics in liquids. From the TRF spectra of both the enol and keto isomers, we have identified the ICT reaction of the keto isomer occurring subsequent to the ESIPT. The ICT proceeds also by two time constants of near instantaneous and 2.7 ps. Since the ICT dynamics of HBOCE is rather close to the polar solvation dynamics, we argue that the ICT is barrierless and determined mostly by the solvent fluctuation.

Introduction

Excited state intramolecular proton transfer (ESIPT) is a phototautomerization occurring in the electronic excited state of a molecule, where a heterocyclic ring is formed by the intramolecular hydrogen bond between a hydroxyl group and a neighboring proton acceptor.[1,2] Recently, a number of functional organic molecules based on ESIPT have been investigated extensively because of their potential applications to optical devices[3−10] as well as the fundamental importance of the proton transfer in chemistry and biology.[11,12] Since a molecule undergoing ESIPT exhibits characteristic photophysical features such as the 4-level reaction scheme, ultrafast reaction within ∼1 ps, and large Stokes shift up to 10 000 cm^{-1}, it can also be exploited as a fast and efficient fluorescence probe, such as laurdan in the biomolecular fluorescence imaging, which utilizes intramolecular charge transfer (ICT).[13,14]

For practical applications of ESIPT systems, a sophisticated modification toward the emission characteristics is essential, which can be achieved by introducing a new functional group to a common ESIPT structure or by changing its environment, such as the polarity of the solvent. Modification of common ESIPT structures (for example, 2-(2′-hydroxyphenyl)benzoxazole (HBO) and its analogs[1,15]) has been widely attempted to produce white-light-emitting materials[6] and molecular probes for biological applications.[16,17] HBO conjugated with an electron-withdrawing group (HBOCE) was developed to increase the Stokes shift even further.[5] The molecular structure and ESIPT scheme of HBOCE are shown in Figure 1. The ESIPT reaction of HBOCE in solution follows the general 4-level reaction scheme. In the ground state, the enol isomer is more stable than the keto isomer, whereas the relative stability is reversed in the excited state. When the enol isomer of HBOCE is excited, it undergoes ESIPT, and the product keto isomer emits with a large Stokes shift. Due to the presence of the electron-withdrawing group, the keto state is strongly affected by the polarity of a solvent, and it may undergo subsequent ICT reaction, as evidenced in their stationary absorption and fluorescence spectra,[5] although dynamics of the ESIPT and ICT processes have not been resolved.

In this work, we have fully characterized the ultrafast ESIPT and subsequent ICT dynamics of HBOCE in solutions and a polymer film by time-resolved fluorescence (TRF) as well as steady-state measurements. It is well-known that TRF is the most intuitive and accurate method for the study of a photoinduced dynamics occurring in an electronic excited state, since TRF probes the excited state dynamics exclusively, whereas the conventional pump/probe transient absorption (TA) may be complicated by the excited state absorptions of reactants and products. TA is also sensitive to the dynamics occurring in the ground state, as well. Since both ESIPT and ICT reactions occur in the excited state and all relevant species show fluorescence at distinct wavelengths, TRF is an ideal tool for the investigation of the dynamics in HBOCE. TRFs for both enol and keto isomers were recorded with a time resolution high enough to resolve the ultrafast ESIPT dynamics unambiguously. In addition, femtosecond TRF spectra for both enol and keto isomers are recorded directly without the conventional spectral reconstruction method to reveal the ESIPT and ICT dynamics separately. Since the dynamics following photoexcitation of HBOCE is

* Corresponding authors: Fax: +82-54-279-8127. E-mail: ketone@postech.ac.kr.
† Department of Chemistry, Pohang University of Science and Technology.
‡ Pohang Accelerator Laboratory, Pohang University of Science and Technology.
§ Seoul National University.

10.1021/jp909438p
Published on Web 04/16/2010

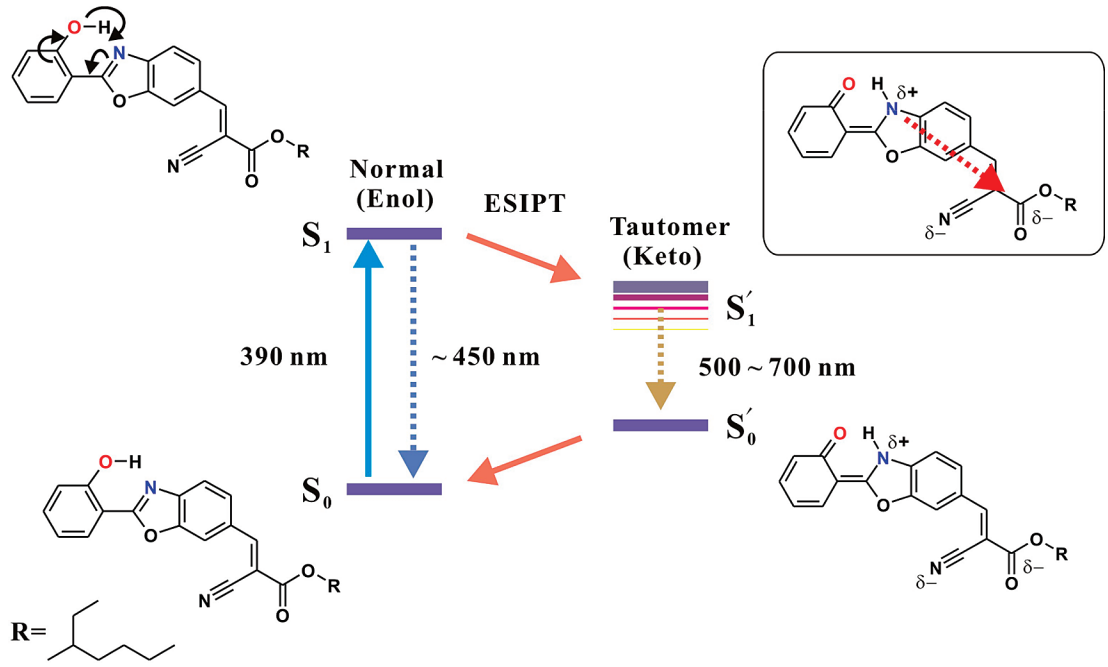

Figure 1. Molecular structure and schematic of the ESIPT and ICT processes of HBOCE in solution.

complicated by the several processes, such as ESIPT, ICT, vibronic relaxation, and solvation, full TRF spectra measurement is required to separate each process by spectral deconvolution. In particular, through the TRF spectra measurements, one can discriminate the ICT following ESIPT from the simple ESIPT reaction, since the dynamic fluorescence Stokes shift of the keto isomer originates mainly from the charge transfer, which is directly coupled with the solvation dynamics.[18]

Experimental Section

Sample Preparation. Synthesis of HBOCE has been reported previously.[5] Cyclohexane, chloroform, acetonitrile, and methanol from Aldrich, and diethyl ether from Fluka were HPLC grade and used without further purification. For TRF experiments, concentrations of HBOCE were adjusted to give absorbance of 0.6 in a 200 μm path length cuvette at the excitation wavelength. To prepare the film sample, HBOCE was dissolved in chloroform and polystyrene with 1:1 weight ratio, spin-coated on a 3-mm-thick optical quality BK7 window and dried under vacuum. Both solution and film samples were installed on a homemade motorized stage to minimize photodamage. All experiments were carried out at ambient temperature (25 °C).

Steady-State Absorption and Fluorescence Measurements. Steady-state absorption spectra of the solution and film samples were recorded by a commercial diode-array spectrophotometer (S-3100, Scinco). Steady-state fluorescence spectra of the solution samples were recorded by a commercial spectrofluorometer (QuantaMaster, PTI). To record the weak emission from the film and methanol solution, a CCD detector (DV-420-0E, Andor) and laser excitation were used.

Femtosecond TRF. The femtosecond light source was a home-built cavity-dumped Ti:sapphire oscillator pumped by a 4.8 W output of a frequency-doubled Nd:YVO_4 laser (Verdi, Coherent). The center wavelength was 780 nm, and the energy of the output pulses was 40 nJ at the repetition rate of 380 kHz. Pump pulses at 390 nm were generated by the second harmonic generation in a 100 μm thick BBO (β-barium borate) crystal. The residual fundamental was used as a gate in the fluorescence up-conversion. Pairs of fused-silica prisms compensate the group velocity dispersions of the pump and the gate pulses. Femtosecond time-resolved spontaneous fluorescence was measured by a noncollinear fluorescence up-conversion technique described elsewhere.[19,20] Briefly, fluorescence was collected by a reflective objective and mixed with the gate pulse in a 500-μm-thick BBO crystal. Polarization of the pump pulse was rotated with respect to the gate pulse by 54.7° using a $\lambda/2$ waveplate for magic angle detection. The fluorescence and the gate were focused to the BBO crystal noncollinearly with an external angle of 20°, where the collaborative effects of the phase front mismatch and group velocity mismatch are minimized. The up-conversion signal was sent to a monochromator and detected by a blue-enhanced photomultiplier tube with a gated photon counter (SR400, Stanford Research System). The instrumental response of the apparatus was estimated to be 100 fs (fwhm) from the cross-correlation between the scattered pump and gate pulses, although the actual time resolutions at the fluorescence wavelengths are significantly better.[19,20] To measure the TRF spectra at a fixed time delay without the conventional spectral reconstruction method, the detection monochromator and the phase matching angle of the BBO crystal were scanned simultaneously. The time delay of the gate pulse was also adjusted simultaneously to compensate the group velocity dispersion arising from the cuvette wall and any imaging imperfection of the apparatus.[21]

Picosecond TRF. TRF at a longer time scale was measured by the time-correlated single photon counting (TCSPC) method. Details of the TCSPC setup has been described elsewhere.[22] A singlet lens was used to focus the excitation beam to the sample, and the subsequent fluorescence was collected in a back-scattering geometry using a parabolic mirror. The emission was sent to a monochromator and detected with a thermoelectrically cooled MCP-PMT (R3809U-51, Hamamatsu). Magic angle detection was used to avoid the effect of polarization. Width (fwhm) of the instrumental response was 40 ps to provide ~10 ps time resolution after deconvolution.

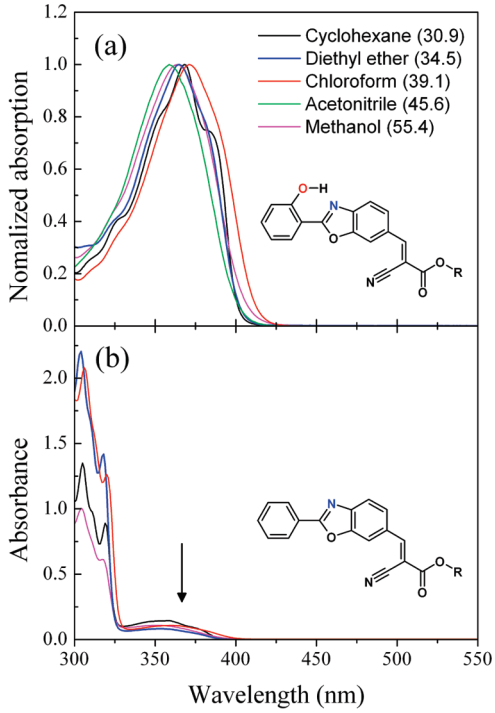

Figure 2. Steady-state absorption spectra of HBOCE (a) and its analog without the hydroxyl group (b) in solution. Numbers in parentheses are the polarity of the solvent in the $E_T(30)$ scale. For the analog, concentrations are 1×10^{-5} M.

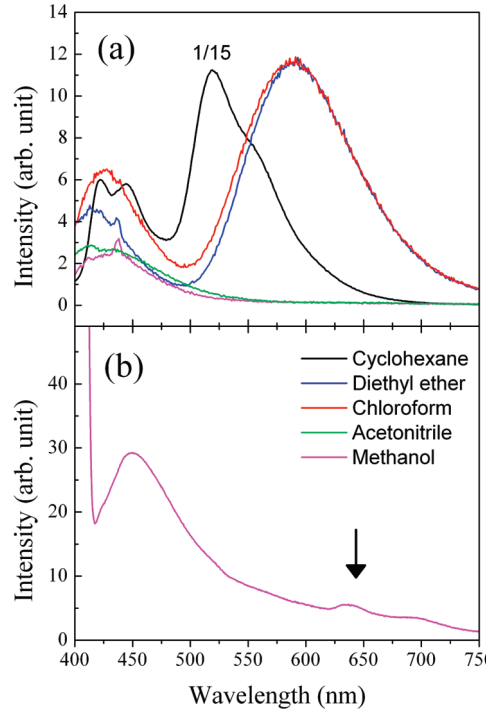

Figure 3. (a) Steady-state fluorescence spectra of HBOCE in solution. Sample concentrations are adjusted to give ~0.3 absorbance at the excitation wavelength of 390 nm. Note that for the cyclohexane, the fluorescence intensity is divided by 15. (b) Steady-state fluorescence spectra of HBOCE in methanol. Arrow indicates the position of the keto emission.

Results

A. Steady-State Absorption and Fluorescence Spectra. Figure 2 shows the steady state absorption spectra of HBOCE and its analog, HBOCE, without the hydroxyl group. In cyclohexane, the absorption maximum appears around 370 nm with apparent vibronic structure. The absorption spectra of HBOCE show slight solvent dependence; the red edge of the absorption band above 400 nm increases monotonically as the solvent polarity increases (the solvent polarity is given by the $E_T(30)$ scale.[23]). Interestingly, however, the absorption maxima in polar solvents do not shift monotonically as the solvent polarity increases; the absorption maximum red-shifts slightly in chloroform, whereas it blue-shifts in diethyl ether, acetonitrile, and methanol. Absorbance of the corresponding band for the analog is much smaller in all solvents (Figure 2b), indicating that the phenyl ring in the analog is not conjugated with the benzoxazole backbone; the absorption spectrum may be described by the two independent absorption bands for each subunit. Therefore, the strong absorption band of HBOCE centered at 370 nm can be accounted for by the reinforced conjugation enabled by the intramolecular hydrogen bond.

Figure 3a shows steady state fluorescence spectra of HBOCE in solutions with 390 nm excitation. According to the reaction scheme shown in Figure 1, the emission band at 430 nm can be assigned to the fluorescence of the enol isomer, and the band in the range of 500−700 nm, to that of the keto isomer. In cyclohexane, vibronic structures are observed in both the enol and keto emission bands at 450 and 570 nm, respectively. One prominent feature of the fluorescence spectra of HBOCE is the rather different Stokes shift values for the polar and nonpolar solvents; Stokes shifts in polar solvents are much larger than that in cyclohexane. Note that a weak keto emission band is observed in acetonitrile at around 650 nm (see Figure S1 in the Supporting Information). This is in strong contrast to the fluorescence spectra of HBO (HBOCE without the electron withdrawing group), which shows nearly the same fluorescence spectra and, thus the same Stokes shifts for both polar and nonpolar (cyclohexane) solvents. In addition, the Stokes shift values of HBO and HBOCE are comparable in cyclohexane. The solvent dependence of the Stokes shifts provides an important clue for the ICT reaction of the keto isomer of HBOCE in polar solvents; that is, the extra Stokes shift of HBOCE in polar solvents may be caused by the charge separation of the keto isomer due to the electron-withdrawing group.

Another notable feature is the absence of the keto emission in methanol. In the previous work, it was concluded, on the basis of the stationary fluorescence spectra, that the ESIPT does not occur in protic solvents, such as methanol.[5] However, the keto emission in methanol solution can be detected by using a CCD array detector (see Figure 3b), revealing that a fraction of HBOCE in methanol forms intramolecular hydrogen bond and undergoes ESIPT. TRF measurements at both enol and keto emission bands give a direct evidence for the ESIPT in methanol (vide infra).

Interestingly, HBOCE in cyclohexane shows a remarkable emission characteristic, as shown in Figure 4a. When the excitation wavelength is tuned to the red edge of the absorption spectrum, the intensity of the keto emission band decreases and becomes undetectable beyond 415 nm excitation. This phenomenon is not observed in the other solvents. Fluorescence excitation spectra were measured to resolve the origin of the emitting state (Figure 4b). When the keto emission is detected, the excitation spectrum is close to the absorption spectrum. When the enol emission is detected, however, an excitation spectrum similar in shape to the absorption but red-shifted is observed. That is, the red-shifted excitation band in 400−450 nm range is responsible for the enol emission exclusively.

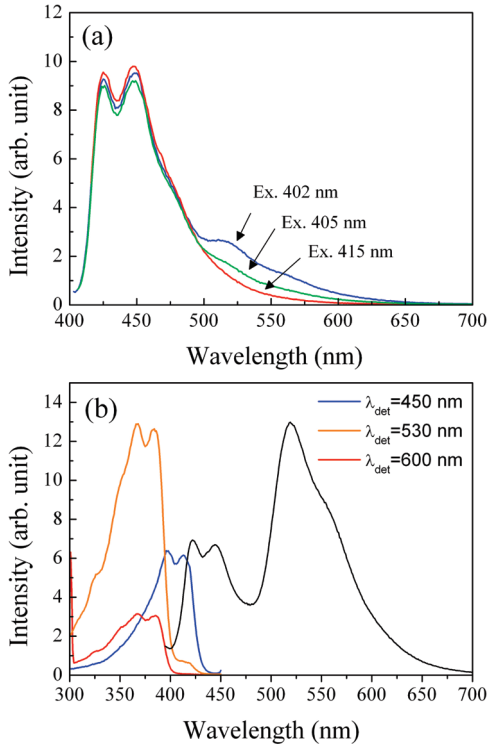

Figure 4. (a) Steady-state fluorescence spectra of HBOCE in cyclohexane by three different excitation wavelengths. (b) Fluorescence excitation spectra with the detection wavelengths at 450, 530, and 600 nm, respectively. Steady-state fluorescence spectrum with 390 nm excitation is also shown by the black solid line.

There may be two possibilities for the rationalization of the anomalous behavior in the fluorescence excitation spectra of HBOCE in cyclohexane. First, it is well-known that HBO exists in equilibrium between two rotational conformers (syn- and antienols) in the ground state.[16,24,25] The molecular structure shown in Figure 1 corresponds to the syn-enol, whereas the phenyl group is rotated by 180° in the antienol to form the hydrogen bond between the hydroxyl group of the phenyl ring and the oxygen atom in the benzoxazole ring. Note that the antienol conformer does not undergo ESIPT.[16,24,25] Thus, one may assign the red-shifted excitation band to the absorption of the antienol conformer that gives the enol fluorescence exclusively. This supposition, however, is not consistent with the absence of the antienol conformer in polar solvents, since the fluorescence of the antienol conformer of the HBO was observed in all solvents.[25] In addition, the center wavelength of the absorption band of the syn-enol conformer is reported to be longer than that of the antienol conformer.[24,26]

Second, several theoretical studies for various ESIPT molecules suggest that excitation to the n−π* state results in the weakening of the hydrogen bond, which is likely to induce the rotation of the hydroxyl group to result in a higher barrier for the ESIPT as compared to the $\pi-\pi$* states.[27−32] In general, as the solvent polarity increases, the energy gap of the $\pi-\pi$* transition decreases, whereas the n−π* transition shows the opposite behavior.[33] Therefore, with the notion of the polarity-induced inversion of the n−π* and the $\pi-\pi$* states, we can justify the anomalous behavior of the fluorescence excitation spectra in cyclohexane. That is, the n−π* state, which shows a higher barrier for the ESIPT reaction, lies below the $\pi-\pi$* state in the nonpolar cyclohexane to show the emission from the n−π* state, whereas the $\pi-\pi$* state is the lowest emissive state in polar solvents.

To verify experimentally the existence of the n−π* state in a nonpolar solvent, we measured the fluorescence quantum yield for the enol emission upon excitation at 415 nm, where the keto emission is not observable. By using Coumarin 47 in ethanol as a standard, which has a fluorescence quantum yield of 0.59,[34] the fluorescence quantum yield of the lowest excited state of the enol form in cyclohexane is measured to be about 2.6×10^{-3}. The radiative lifetime is calculated to be about 280 ns from the actual lifetime of 725 ps measured from a picosecond TRF experiment (vide infra). It is well-known that an n−π* transition in common organic molecules has a small oscillator strength to give a radiative lifetime longer than 100 ns.[35] Therefore, in contrast to the polar solvents, we can assign the lowest emissive state of the enol form in cyclohexane to the n−π* state.

B. Time-Resolved Fluorescence at Fixed Wavelengths. Figures 5 and 6 show picosecond and femtosecond TRF signals of HBOCE in solutions, respectively, measured at several fixed wavelengths. Exponential fit results are listed in Table 1. In the picosecond TRF, we observe an instrument limited decay at the enol emission wavelength and the corresponding rise at the keto emission wavelength, indicating that the ESIPT dynamics is ultrafast in solution. These results are consistent with the femtosecond TRFs at 450 and 650 nm using the up-conversion method that shows the ultrafast decay and rise components within 2 ps. Interestingly, a 725 ps slow decay component at the enol emission is observed for the cyclohexane solution, in addition to the ultrafast decay component in the picosecond TRF. These results are consistent with the steady-state fluorescence spectra, in which only the HBOCE in cyclohexane shows the n−π* emission at 450 nm.

For all solution samples, the femtosecond TRF signals measured near the center (570−600 nm) of the keto emission spectra show an instantaneous rise component, followed by relatively slow rise and decay components. The instantaneous rise is due to the contamination from the enol emission and should not be confused with the ultrafast ESIPT reported for a rigid and coplanar ESIPT molecule showing extremely fast ESIPT within 20 fs.[36,37] The fluorescence spectra of the enol isomers show a long tail. Moreover, the oscillator strength responsible for the enol emission should be much larger than that of the keto emission, since the intensities of the enol emissions are comparable to those of the keto emissions, even though their lifetimes (~1.5 ps) are much shorter.

As indicated above, the ultrafast ESIPT dynamics can be resolved by femtosecond TRF measurement. The femtosecond TRF signals measured at the enol emission (450 nm) show at least two time constants of a few hundred femtoseconds and about 1.5 ps (see Table 1) in all solvents. In cyclohexane, for which the ESIPT dynamics is not complicated by the ICT of the keto isomer, two rise components corresponding to the decay at the enol emission wavelength are clearly resolved at the keto emission of 650 nm, suggesting that at least two different ESIPT dynamics should exist for the syn-enol isomer in solution. We recently reported the ESIPT dynamics of a semirigid polyquinoline in solution and polymer film.[38] Strong dispersion of the ESIPT rates was observed in liquid but not in film, which was accounted for in terms of the conformational heterogeneity along the dihedral angle between the proton donor and the acceptor groups.[38] Similarly, conformational heterogeneity due to the dispersion of the dihedral angle between the phenyl and benzoxazole groups may bring about the nonexponential dynamics; the faster decay component originates from the ESIPT reaction of a nearly planar syn-conformer, in which low-

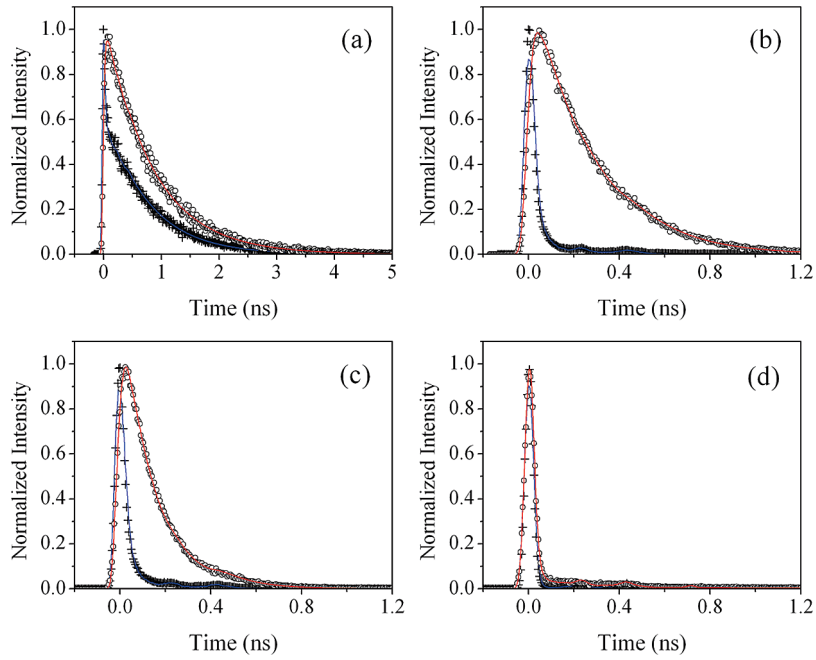

Figure 5. Picosecond time-resolved fluorescence signals of HBOCE in cyclohexane (a), diethyl ether (b), chloroform (c), and methanol (d) detected at 450 nm (cross) and 610 nm (circle). Solid lines represent the exponential fits.

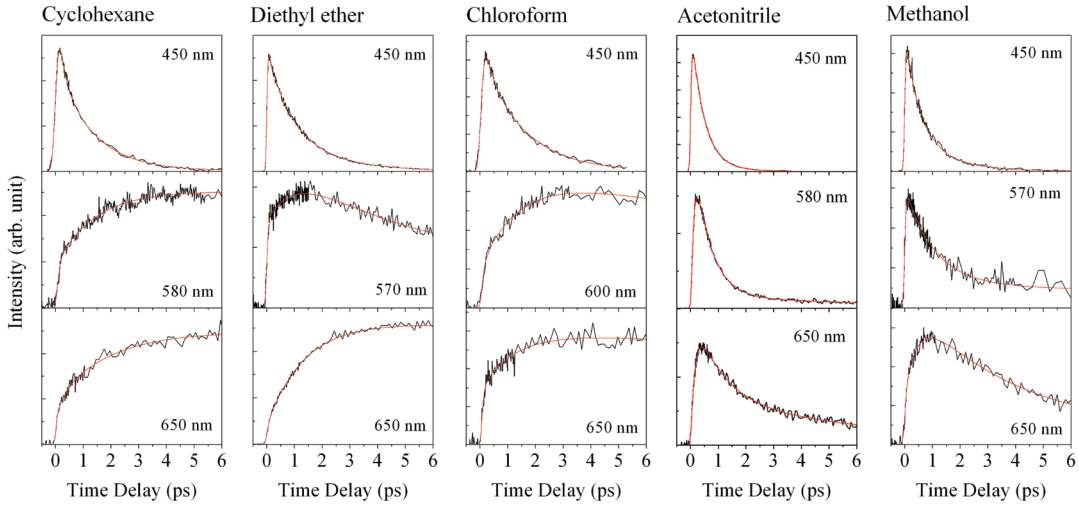

Figure 6. Femtosecond time-resolved fluorescence signals of HBOCE in solution. Exponential fits are overlaid on the signals.

frequency skeletal motions may act as a reaction coordinate,[36,39−41] whereas the second slow decay component originates from a twisted syn-conformer. It is well-known that a broad conformational distribution of a molecule in the ground state originating from a flexible molecular structure in a less confined environment, such as liquid, can give a dispersion of the reaction rates.[38,42,43]

The slower ESIPT time in the range of 1−2 ps is similar to the time scale of the internal rotational motion of the phenyl ring,[17,44] which indicates that the twisting motion of the proton donor group may participate in the ESIPT. To examine the idea that a rigid environment may suppress the slower ESIPT process via torsional motions, we have investigated the ESIPT dynamics of HBOCE in a polymer film. Figure 7 shows steady-state absorption and fluorescence spectra and TRF signals of HBOCE in the poly styrene film. Compared with the steady-state fluorescence spectra of HBOCE in solutions, the intensity of the enol emission is greatly reduced, implying a faster ESIPT rate in the polymer film. This phenomenon is demonstrated by the TRFs as shown in Figure 7b and c, in which the fast decay component of the enol emission is dominant (see Table 1). These results suggest that the rotational motion of the bulky donor group acts as a reaction coordinate and is responsible for the slower ESIPT rate. Similar results were observed for the ESIPT dynamics of 2-(2′-hydroxyphenyl)-4-methyloxazole (HPMO) in a rigid environment.[17]

The lifetime of the keto isomer is highly solvent-dependent. In particular, the first decay time constants (τ_2) at 650 nm are much shorter in acetonitrile (1.0 ps) and methanol (3.4 ps) than those in other solvents, indicating that the absence of the keto emission in the steady-state fluorescence is not due to the lack of ESIPT, but is mainly due to the fast nonradiative decay of the keto isomer (or ICT state). Therefore, we can conclude that the ESIPT of HBOCE in methanol is, indeed, probable.

The fastest ESIPT time (τ_1) in the range of 200−800 fs seems to depend much on the solvent properties, such as the polarity and viscosity. However, we cannot firmly determine

TABLE 1: Nonlinear Least-Square Fit Results for the Time-Resolved Fluorescence Signals[a]

	λ (nm)	A_1	τ_1 (fs)	A_2	τ_2 (ps)	A_3	τ_3 (ps)[b]
cyclohexane	450	0.38	230	0.62	1.3	<0.01[c]	730
	580	−0.18	90	−0.32	1.4	0.5	820
	650	−0.10	260	−0.34	2.0	0.56	820
diethyl ether	450	0.60	810	0.40	1.8		
	570	−0.35	960	0.46	3.5	0.19	220
	650			−0.46	1.3	0.54	180
chloroform[d]	450	0.18	200	0.35	1.5		
	580	−0.23	810	0.5	25	0.1	130
	650			−0.24	1.3	0.46	130
acetonitrile	450	0.93	450	0.07	1.6		
	580	−0.53	100	0.44	0.6	0.03	160
	650	−0.50	160	0.33	1.0	0.17	160
methanol	450	0.76	550	0.24	1.4		
	570			0.75	1.1	0.25	90
	650	−0.39	480	0.52	3.4	0.085	90
film	450	0.69	490	0.31	3.0		
	580	−0.18	480			0.82	210

[a] Negative amplitudes indicate rise components. [b] In acetonitrile, the last components (τ_3) were measured by the fluorescence up-conversion. In the other solvents, time constants longer than 50 ps were measured by TCSPC, and they were used in the fitting of the up-conversion signals by fixing them. [c] Amplitude of the τ_3 component was negligible in the fluorescence up-conversion signal at 450 nm. [d] Rise component of about 50 fs was observed at all wavelengths.

the effect of the solvent from the TRFs detected at individual wavelengths. Actually, the time constants obtained from the TRFs at a single wavelength cannot accurately represent the ESIPT rate because they are strongly affected by the subsequent ICT and spectral relaxation processes, such as solvation and vibronic relaxation. Therefore, the time constants listed in Table 1 should be viewed only as approximate time scales. In this case, examination of the overall time evolution of the TRF spectra should be the most intuitive and robust method. In fact, we have successfully identified two time constants of 250 fs and 1.2 ps for the ESIPT of HBOCE for all solutions, different from the scattered time constants in Table 1, by analyzing the spectrally integrated intensities of the TRF spectra (vide infra).

C. Time-Resolved Fluorescence Spectra Measurements. The ICT dynamics of the nascent keto isomer cannot be resolved clearly by the TRF at individual wavelengths, although the second rise component of the emission at 650 nm may be assignable to the ICT time. Measurements of the TRF spectra over the whole emission wavelength range should be performed to elucidate the subsequent ICT dynamics and the solvation of the ICT state. Figure 8 shows the TRF spectra in the enol emission region of HBOCE in five different solvents. Time evolutions of the TRF spectra exhibit common features in all solvents. First, the TRF spectra broaden significantly in a few hundred femtoseconds and decrease in intensity in about 2 ps by the ESIPT reaction. This is an indication that the ESIPT reaction dynamics of HBOCE in solution does not depend much on the solvent properties For methanol, the TRF spectra before 100 fs could not be measured because of the stray light. Nonetheless, the features of the enol spectra after 100 fs are the same as the other samples, indicating that HBOCE undergoes ESIPT, even in methanol.

Second, although the characteristic solvation times for diethyl ether, chloroform, acetonitrile, and methanol are 2.4 ps, 2.8 ps, 260 fs, and 5.0 ps, respectively,[45,46] dynamic Stokes shifts of the enol emission spectra by solvation dynamics

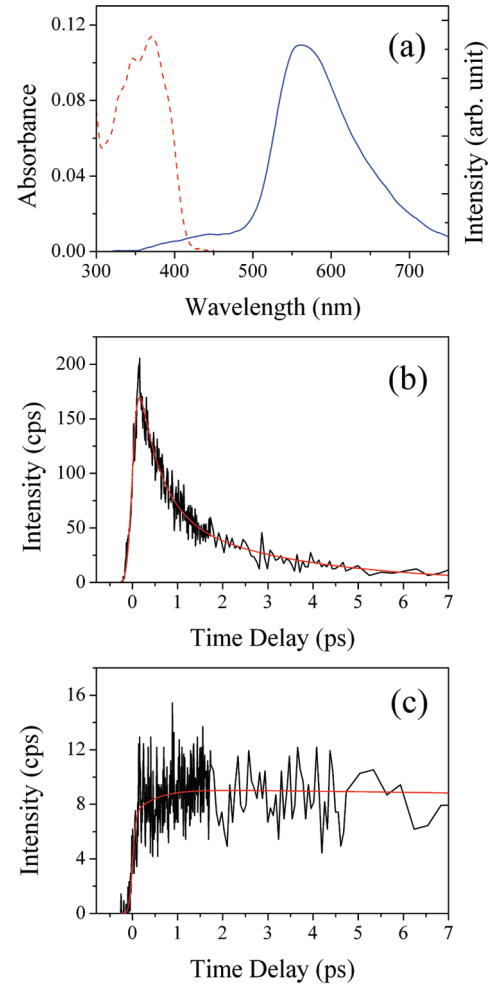

Figure 7. (a) Steady-state absorption (red dashed line) and fluorescence (blue solid line) spectra of HBOCE in polystyrene film. (b, c) Femtosecond fluorescence signals measured at 450 and 580 nm, respectively. Red lines represent the exponential fits.

are not observable up to 4 ps, which indicates that the dipole moment change between the ground and excited states is negligible in the enol isomer and that the ICT do not occur in the excited state of the enol isomer. Third, a rise around 540 nm in the TRF spectra, which corresponds to the generation of the keto isomer, is not well-resolved from the strong enol emission band centered at ∼430 nm, since the oscillator strength of the keto isomer is much smaller than that of the enol isomer.

The spectral broadening at early times can be accounted for by the dephasing of the coherent nuclear wave packets created in the excited state of the enol isomer. The wave packet generated initially by the impulsive excitation is localized to give a narrow spectrum, and then it undergoes a dephasing process during the ESIPT reaction. In addition to the broadening, the TRF spectra in cyclohexane, diethyl ether, and acetonitrile show ultrafast blue shifts in 100 fs, whereas the ultrafast blue shift is not observed for HBOCE in chloroform, although the origin of the ultrafast blue shift in the TRF spectra is not clear.

Accurate determination of the ESIPT rate free from the spectral evolution, such as the blue shifts and broadening of the TRF spectra, is critical for the correct description of the reaction mechanism. Within the Condon approximation, spectrally integrated intensity of the TRF spectra should be directly proportional to the population of the enol isomer in the excited

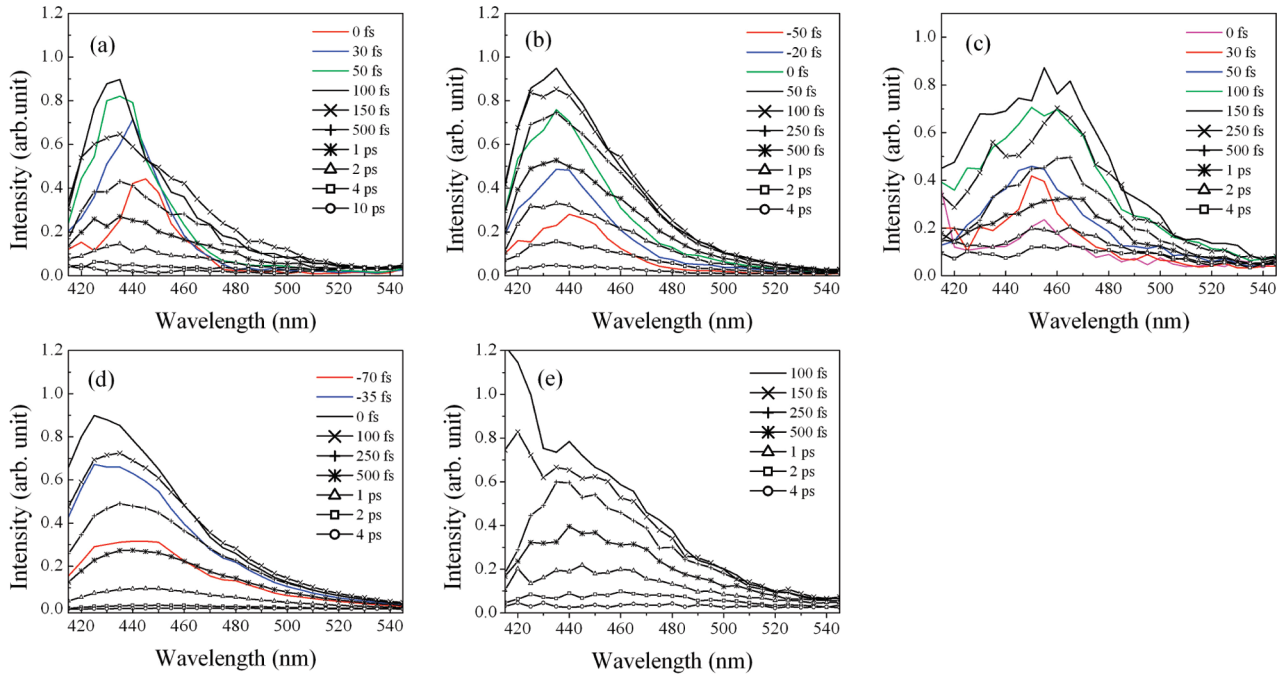

Figure 8. Time-resolved fluorescence spectra for the enol emission of HBOCE in cyclohexane (a), diethyl ether (b), chloroform (c), acetonitrile (d), and methanol (e). In methanol, there is a strong stray light at 420 nm within 100 fs time delay.

state, whose major decay channel is the ESIPT reaction. We analyzed the area of each TRF spectrum by fitting it to a log-normal function

$$\begin{aligned} f(\nu) &= h\exp\left[-\ln(2)\left(\frac{\ln(1+\alpha)}{\gamma}\right)^2\right] && \alpha > -1 \\ &= 0 && \alpha \le -1 \end{aligned} \tag{1}$$

where

$$\alpha = \frac{2\gamma(\nu - \nu_0)}{\Delta}$$

Here, h, ν_0, Δ, and γ are peak height, peak frequency, width, and asymmetry parameter, respectively. For the cyclohexane, acetonitrile, and diethyl ether solutions, a single log-normal function was used to fit the TRF spectra, whereas an additional function was included for the chloroform and methanol solutions to subtract the background from stray light (nonlinear least-squares fit results are shown in Figure S2 in the Supporting Information). The area of the log-normal function at a time delay t is

$$I(t) = h(t)\left(\frac{\pi}{4\ln(2)}\right)^{1/2}\Delta(t)\exp\left(\frac{\gamma(t)^2}{4\ln(2)}\right) \tag{2}$$

Figure 9 shows the spectrally integrated intensity, $I(t)$. Two exponential fits for the decay of $I(t)$ for each solution of HBOCE were obtained from the global analysis of the set of TRF spectra, and the fit results are also shown in Figure 9. It is remarkable that $I(t)$ for all solutions is well-described by two exponential functions with the same time constants of 250 fs and 1.2 ps. Moreover, relative amplitudes of the two components are similar for all solvents, with the 1.2 ps component being the major ESIPT channel ($A_2/A_1 \sim 2$) except for acetonitrile, for which the 250 fs component is dominant ($A_2/A_1 \sim 0.15$). The fact that the ESIPT dynamics is similar in different solvents but qualitatively different from that in a rigid environment introduced by the polymer film leads to the notion that the ESIPT dynamics of the HBOCE depends much on the molecular conformation, which is affected mostly by the rigidity of the environment. The irregularity for acetonitrile cannot be accounted for by the solvent polarity alone, since only the amplitude ratio (A_2/A_1) changes dramatically in acetonitrile, whereas it is close to 2 even in methanol having a higher polarity. It is interesting to note that the absorption maxima of HBOCE in diethyl ether and methanol are similar but that in acetonitrile blue-shifts farther, which may imply a stronger interaction between HBOCE and acetonitrile in the ground state to induce a certain molecular conformation that is favorable for the ultrafast ESIPT.

To elucidate the ICT and its dynamics of nascent keto isomer subsequent to the ESIPT, we measured TRF spectra in the keto emission region for the two solvents cyclohexane and diethyl ether, which have distinct polarities. Figure 10 shows the TRF spectra in the range of 520 to 670 nm. Spectral evolutions of the TRF spectra in the two solvents are entirely different, demonstrating that the ICT reaction is, of course, strongly solvent-polarity-dependent. In cyclohexane, the TRF spectra can be well-described by the sum of the strong enol emission and the keto emission centered at around 525 nm, which appears as a weak shoulder. At time zero, the keto emission cannot be observed. This is consistent with the TRF spectra for the enol emission at time zero (Figure 8a), where the enol spectrum in cyclohexane is highly localized at the Franck−Condon region to give no keto emission at time zero.

As the time increases, the contribution of the enol isomer decreases, and the keto emission becomes a separate band after ~5 ps. It is important to note that the TRF spectra of the keto isomer do not red-shift, and only a weak vibronic band at 570 nm develops with a time constant of a few hundred femtoseconds. The TRF spectra clearly show that the keto isomer does not undergo ICT reaction in nonpolar cyclohexane. In diethyl

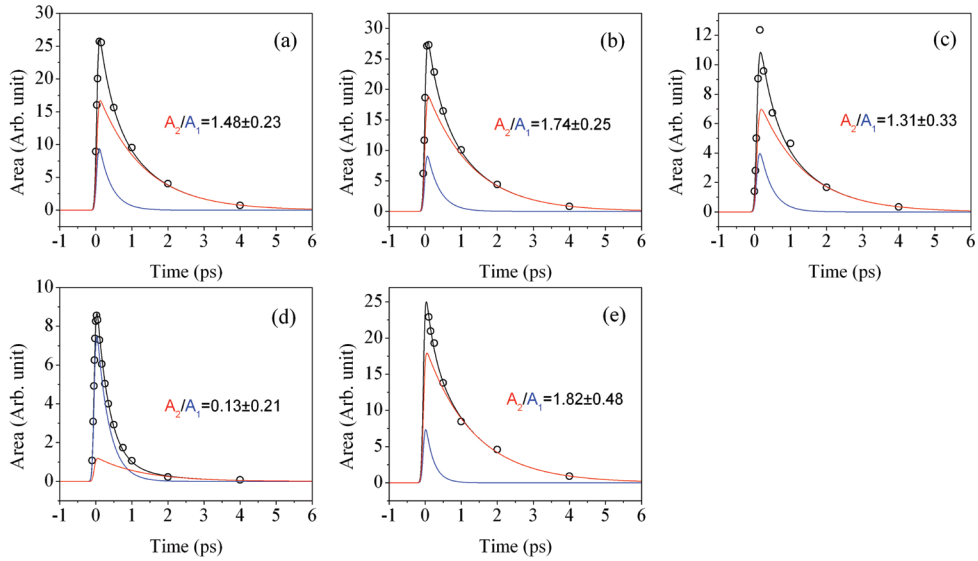

Figure 9. Spectrally integrated intensities of the time-resolved fluorescence spectra for the enol emission of HBOCE in cyclohexane (a), diethyl ether (b), chloroform (c), acetonitrile (d), and methanol (e). Two exponential fits are overlaid to the data, and each exponential component is shown by the red and blue lines.

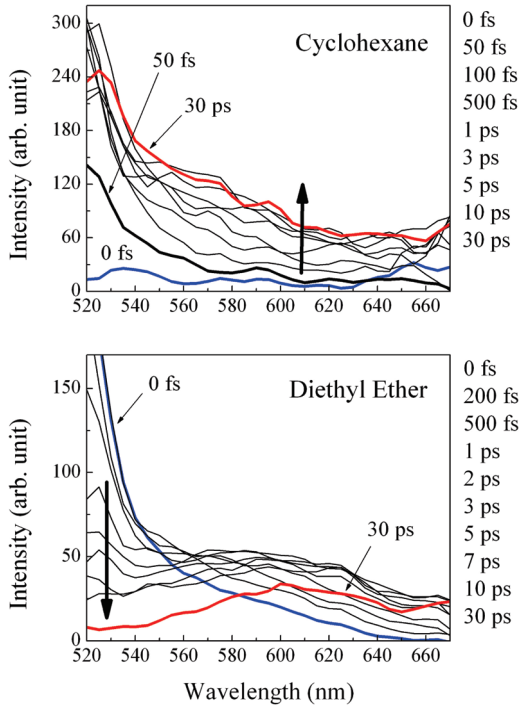

Figure 10. Time-resolved fluorescence spectra for the keto emission region of HBOCE in cyclohexane and diethyl ether. Arrows indicate the order of time delays listed on the right side of each panel.

ether, however, an emission band around 570 nm is clearly observed, even at time zero. As time increases, the intensity of the enol emission band decreases, and the emission band around 570 nm increases while it undergoes dynamic Stokes shift. Since it undergoes dynamic Stokes shift only in a polar solvent, the band around 570 nm can be regarded as the emission from the ICT state of the keto isomer.

The overall experimental results support the reaction pathway shown in Scheme 1, where E*, K* and K^*_{CT} denote syn-enol, syn-keto, and the ICT states of the syn-keto, respectively, in their excited states. At time zero, center wavelengths of the E*, K*, and K^*_{CT} emission bands should be around 450, 525, and 570 nm, respectively. From the TRF spectra of the enol isomer, it was shown that HBOCE in solutions undergoes ESIPT with two time constants, 250 fs and 1.2 ps. The nascent K^*_{CT} subsequently undergoes solvation. It is important to note that solvation dynamics of the most polar solvents shows a bimodal behavior: an ultrafast (~100 fs) component attributed to the inertial motion and a few picosecond components for the diffusive motion of solvents (2.4 ps for diethyl ether).[45,46] The ICT reaction is often directly coupled with the solvent coordinate so that it is driven by the solvent fluctuations, as observed for some electron transfer reactions.[47−49] That is, the ICT rate may be similar to the time scales of the polar solvation dynamics. The TRF spectrum at time zero for the keto emission in diethyl ether shows a red-shifted band, which undergoes fast solvatochromic shift within a few picoseconds. In fact, this result is consistent with the reaction Scheme 1 along with the solvation-driven ICT dynamics.

We have performed global analysis of the TRF spectra according to Scheme 1 with the dynamic Stokes shift of K^*_{CT}. Each species is represented by a log-normal function, and the integrated intensities $I(t)$ for each species at time t is calculated by eq 2. In the fitting, vibronic relaxation of the nascent K*, the time scale of which may be in the range of 200−400 fs,[36,37] is not considered because of its minor effect on the TRF spectra. Furthermore, some parameters of the log-normal functions are constrained according to the results from the stationary and time-resolved studies to remedy the instability in the fitting due to the spectral congestion. For E*, amplitude of the log-normal function is varied biexponentially with time constants of 250 fs and 1.2 ps, while the other three parameters ν_0, Δ, and γ are fixed to 22 222 cm^{-1}, 1500 cm^{-1}, and −0.4, respectively. For K*, ν_0, Δ, and γ are fixed to 19 048 cm^{-1}, 1500 cm^{-1}, and −0.4, respectively. For K^*_{CT}, the parameters are allowed to vary single exponentially to account for the dynamic Stokes shift and the spectral broadening:

$$\begin{aligned} \upsilon_{0,K^*_{CT}}(t) &= \upsilon_0(\infty) + \delta\upsilon \times \exp(-t/\tau) \\ \Delta_{K^*_{CT}}(t) &= \Delta(0) + \delta\Delta \times (1 - \exp(-t/\tau)) \\ \gamma_{K^*_{CT}}(t) &= -\gamma(\infty) - \delta\gamma \times \exp(-t/\tau) \end{aligned} \quad (3)$$

SCHEME 1: Bimodal ESIPT and Solvation-Driven ICT Reactions of HBOCE in Solution

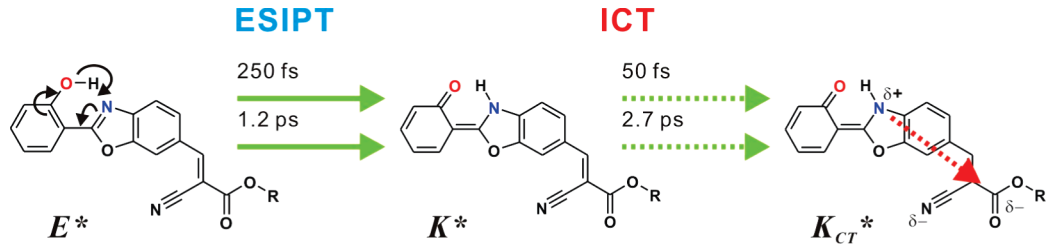

where τ is a time constant for the dynamic Stokes shift and spectral width change by solvation dynamics. From the global analysis with the constraints above, we successfully extracted the TRF spectra of the K* and K^*_{CT}. Some examples of the global fit results are shown in Figure 11.

Global fit results for the K^*_{CT} are listed in Table 2. The time constant for the dynamic Stokes shift of K^*_{CT} from the fit is 2.7 ps, which is close to the diffusive solvation time of diethyl ether (2.4 ps).[50] It should be noted that this value is different from the rise component of 1.3 ps obtained from the single wavelength TRF at 650 nm. Figure 12 shows the spectrally integrated intensities, $I(t)$, of two keto isomers, K* and K^*_{CT}, from the fit. For comparison, analytic solutions for the K* and K^*_{CT} according to Scheme 1 are calculated using the parameters from the global fit, and they are also shown in Figure 12. The relative amplitudes of the 250 fs and 1.2 ps components in the ESIPT dynamics are fixed to 1:1.74 according to the TRF spectra result (see Figure 9b).

For the ICT dynamics in diethyl ether, two ICT rates of $(50\ \text{fs})^{-1}$ and $(2.7\ \text{ps})^{-1}$ are included in Scheme 1. Note that the formation rate of K^*_{CT} at early times should be determined by that of the K* because of the relatively slow ESIPT time of 250 fs as compared to the faster $(50\ \text{fs})^{-1}$ ICT rate. Rate equations for the K* and K^*_{CT} are solved by the determinant method.[51] The analytic simulation results including the two ICT processes with equal amplitudes reproduce the experiments very well.

Overall kinetic simulations together with the corresponding experimental results demonstrate that the ESIPT and subsequent ICT dynamics of HBOCE in the polar solvent diethyl ether can be well-described by Scheme 1. Moreover, the ICT dynamics is quite similar to the solvation dynamics, suggesting that the ICT reaction is driven by the polar solvation process, in which the solvation dynamics consists of a nearly instantaneous component (50 fs) attributable to the inertial dynamics and a relatively slow component (2.7 ps) for the diffusive dynamics with equal amplitudes.

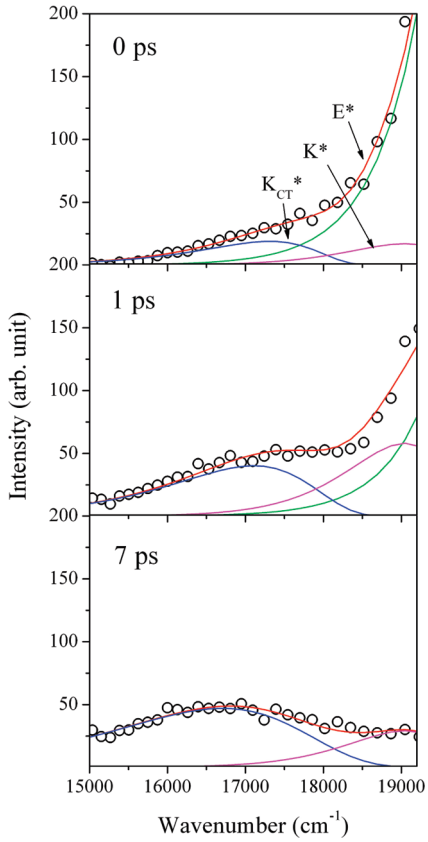

Figure 11. Representative global fit results of the time-resolved fluorescence spectra for the keto emission of HBOCE in diethyl ether. E*, K*, and K^*_{CT} denote the excited enol, keto, and charge transferred keto states, respectively.

TABLE 2: Global Fit Parameters for the Time-Resolved Fluorescence Spectra of the ICT Band (K^*_{CT}) in Diethyl Ether

time constant	center frequency		width		asymmetry parameter	
τ, ps	$\nu_0(\infty)$, cm^{-1}	$\delta\nu$, cm^{-1}	$\Delta(0)$, cm^{-1}	$\delta\Delta$, cm^{-1}	$\gamma(\infty)$	$\delta\gamma$
2.69 ps	16660	654	1718	1213	0.39	0.13

Discussion

In this work, we have examined the proton transfer and subsequent charge transfer dynamics of HBOCE in solutions

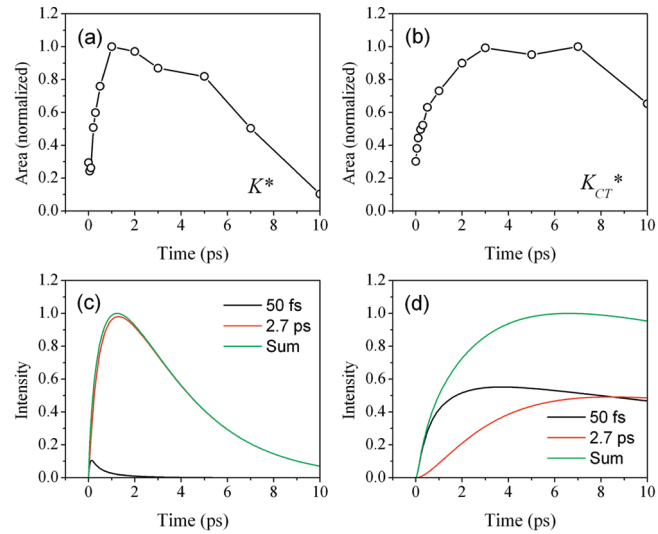

Figure 12. Integrated intensities of the K* (a) and K^*_{CT} (b) obtained by the global fits described in the text. Simulation results for the K* (c) and K^*_{CT} (d) in diethyl ether according to Scheme 1. In the simulation results, two ICT components with reaction times of 50 fs and 2.7 ps are also shown separately, as well as the sum of the two.

and film occurring in electronic excited states by means of steady-state and time-resolved spectroscopies. Through the TRF spectra as well as the TRF at the fixed wavelengths, we have successfully resolved the two ultrafast and sequential dynamics occurring in the excited state and proposed that the conformational heterogeneity in the ground state determines the overall reaction dynamics.

In the ground state, we expect three different conformers: syn-enol, antienol, and solvated enol isomers. Wang et al. reported that the antienol emission of HBO is negligible in cyclohexane (2% of the keto emission).[25] In polar solvents, however, it was reported to be comparable to the emission of the solvated syn-enol isomer, and the solvated enol isomers of HBO in alcoholic solvents show an intense emission with their lifetimes of a few hundred picoseconds.[25] The antienol form of HBOCE may exist in all solvents, but we do not resolve any decay component responsible for that in the TRF experiments. Only the emission from the n$-\pi^*$ state is resolved in nonpolar solvent to give a slow decay component of 725 ps. The absence of the antienol emission suggests that the energetics of the syn- and antienol isomers in the ground state for HBOCE is somewhat different from that for HBO. To investigate the relative population of the two isomers in the ground state, we have performed quantum mechanical calculations for both syn-enol and antienol isomers by using the Gaussian 03W package with the DFT (B3LYP/6-31G(d)) method.[52] The calculated energy of the syn-enol is lower by 1972 cm^{-1} than that of the antienol isomer, and dipole moments of the syn- and antienol isomers are 4.46 and 5.74 D, respectively. The theoretical results indicate that the population of the antienol conformer of HBOCE in the ground state is negligible and that the antienol isomer may be less stabilized in nonpolar solvent. Although solvated enol isomer may be expected in protic solvent such as methanol, we do not observe any slow decay component in the TRF of the methanol solution, which indicates that either the population to the solvated enol isomer is negligible or nonradiative decay of the excited solvated enol isomer is faster than (or comparable to) the time scale of the ESIPT.

We argued that the lowest excited state of the HBOCE enol isomer in cyclohexane is n$-\pi^*$. Theoretical studies on model compounds predicted that the n$-\pi^*$ state lies close to the $\pi-\pi^*$ state so that effective vibronic coupling between the two states may induce internal conversion between them.[27−32] Several time-resolved experiments on ESIPT systems supported the prediction: Chou and co-workers reported that the lowest excited state of the 3-formyl-7-azaindole complex should be in the n$-\pi^*$ configuration and the internal conversion between two states occurs on a time scale should be less than a few hundred femtoseconds, thereby in competition with the ESIPT.[31,53] Okabe et al. also reported a similar result for the *N*-salicylideneaniline molecule.[54] For HBOCE, we may need to consider this process together with the ESIPT processes showing biexponential behavior in all solvents. In polar solvents, however, we found that the generation of the n$-\pi^*$ state is not probable because femtosecond and picosecond TRF signals of the enol emission in polar solvents did not show any components for the n$-\pi^*$ emission. Furthermore, the internal conversion between the two states may be negligible, even in cyclohexane, because ESIPT shows bimodal behavior with the same time constants in all solvents, including cyclohexane, which indicates that the observed n$-\pi^*$ emission upon the excitation of 390 nm is due to direct excitation to the n$-\pi^*$ state caused by the broad spectral width of the pump pulse.

Two distinct time scales (250 fs and 1.2 ps) for the ESIPT of HBOCE are revealed by femtosecond TRF experiments. In a recent report by Chou and co-workers,[55] however, an HBO derivative showed somewhat different dynamics, although it has a similar molecular structure; that is, HBO with an electron-withdrawing moiety having two cyano groups (diCN-HBO). It shows a single exponential ESIPT dynamics, whereas the rate in solution depends on the solvent polarity; 1.1 ps and 300 fs for cyclohexane and acetonitrile solutions, respectively.[54] For HBOCE, however, the ESIPT rate is independent of the solvent polarity, indicating that the ESIPT rates are determined essentially by the attributes originating from the molecular properties alone, not by the solvent-related characteristics such as the reaction barrier that is modulated by the solvent polarity. Thus, we argue that more than one distinct molecular conformation in solution for this flexible molecule HBOCE may lead to the solvent independent bimodal reaction dynamics. The electron-withdrawing group may also affect the charge density of HBOCE to reduce the hydrogen bonding strength between the proton donor and acceptor groups, which may result in more flexibility in the dihedral angle around the hydrogen bond. Note that an extremely fast single exponential ESIPT time constant of about 13 fs was reported for a rigid molecule, 10-hydroxybenzo[*h*]quinoline (HBQ), and the ESIPT time constant was lengthened to 60 fs for a relatively less rigid molecule, 2-(2′-hydroxyphenyl)benzothiazole (HBT).[37] All these results point to the importance of the conformational aspect on the ESIPT dynamics, and distinct molecular conformations should be considered for the ESIPT reactions in nonrigid molecular systems.

Altough the slow 1.2 ps component can be assigned to the ESIPT reaction channel involving twisting motions of the proton donor group, the fast 250 fs component should be related to the ESIPT in a planar structure, and the reaction coordinate may correspond to the low-frequency skeletal motions that prompt the proton transfer without reaction barrier. Wang et al. reported that the ESIPT dynamics of the HBO in cyclohexane is characterized by the 150 fs single exponential determined from the enol emission.[25] Lochbrunner et al. also reported a similar time scale for the same molecule measured by transient absorption with 30 fs time resolution.[41] They observed coherent wavepacket oscillations at the stimulated emission of the product keto isomer and argued the role of the low-frequency skeletal vibrations as reaction coordinates. Although the time resolution is fast enough to observe oscillations in the TRF signal below $\sim$200 cm^{-1}, we do not observe such wave packet dynamics at the keto product emission wavelengths because of the slow reaction as compared with the vibrational time scale, which indicates a reaction barrier for the ESIPT of HBOCE, in strong contrast to the ESIPT of similar molecules without the electron withdrawing group.

Direct measurements of the TRF spectra for both excited enol and keto states reveal that HBOCE in polar solvent undergoes the proton transfer and charge transfer sequentially in that order, as can be seen in Figure 12. Moreover, the charge transfer dynamics follows the solvation dynamics closely,[56] which suggests that the ICT reaction may be driven by the solvent fluctuations, as observed for some electron transfer reactions in the context of the Sumi/Marcus model,[57] in which the free energy barrier between the excited keto state and the ICT state is negligible, to induce the fast dynamics via stochastic solvent motions.[18] Many molecular systems showing intramolecular proton transfer as well as intramolecular charge transfer have been investigated previously to reveal their dynamics and the coupling of the proton transfer and charge

transfer.[58−63] In strong contrast to the present result, most studies reported that the charge transfer occurs prior to the proton transfer. Notably, Chou and co-workers reported that diCN-HBO and 2-{[2-(2-hydroxyphenyl)benzo[*h*]thiazol-6-yl]methylene}malononitrile (diCN-HBT), which are structurally very similar to HBOCE, undergo proton transfer and charge transfer simultaneously, but the ESIPT is strongly coupled with the solvent polarization.[55] Indeed, the charge transfer and proton transfer dynamics are rather sensitive to small perturbations on the molecular structure. For the HBOCE employed in this work, the ESIPT and ICT reactions might also be coupled. Moreover, since both the ESIPT and ICT dynamics are bimodal in liquid and their time scales are also very close, study of their dynamics is quite involved. In this work, the TRF spectra measurement over the entire emission wavelength with high time resolution clearly establishes the dynamics. The instantaneous rise of the enol emission spectra (see Figure 9), independence of the decay of the enol emission on solvents, and the absence of the dynamic Stokes shift of the enol emission band demonstrate unambiguously that the ESIPT occurs prior to the ICT process and that the excited enol does not carry the charge transfer character. Spectral decomposition into the enol, keto, and ICT emission bands through the global analysis of the emission spectra substantiate this conclusion.

Conclusion

We have investigated ESIPT and ICT dynamics of HBOCE in solution and polymer film phases by time-resolved fluorescence and direct TRF spectra measurements without relying on the spectral reconstruction method. First of all, we established that population of the antienol conformer in the ground state is negligible and that the ESIPT occurs in all solvents employed here, including the protic solvent methanol. Subsequent to the ESIPT, ICT occurs in polar solvents, which can be verified by the dynamic Stokes shift of the ICT state emission. The ESIPT dynamics of HBOCE is independent of the solvent and shows a bimodal behavior with the time constants of 250 fs and 1.2 ps components. We argue that conformational heterogeneity in the ground state originating from the dispersion of the dihedral angle that forms the intramolecular hydrogen bond may account for the dispersive ESIPT dynamics in liquids. From the quantitative analysis of the TRF spectra, we showed that the nascent keto isomer also undergoes the ICT dynamics by two time constants of near instantaneous and 2.7 ps, which are rather close to the solvation dynamics in solution, indicating that the ICT reaction has negligible reaction barrier and the rate is determined mostly by the solvent fluctuation.

Acknowledgment. This work was supported by the Basic Science Research Program through a National Research Foundation of Korea (NRF) grant funded by the Korean Government (MEST) (R11-2007-012-01001-0), a NRF grant (2009-0081132), and in part by a Korea Research Foundation grant funded by the Korean Government (KRF-2008-314-C00167).

Supporting Information Available: Steady-state fluorescence spectrum of HBOCE in acetonitrile is shown in Figure S1. Nonlinear least-squares fit results of the TRF spectra in the enol emission region are shown in Figure S2. This information is available free of charge via the Internet at http://pubs.acs.org.

References and Notes

(1) Ormson, S. M.; Brown, R. G. *Prog. React. Kinet.* **1994**, *19*, 45.
(2) Douhal, A.; Lahmani, F.; Zewail, A. H. *Chem. Phys.* **1996**, *207*, 477.
(3) Costela, A.; Garcia-Moreno, I.; Mallavia, R.; Amat-Guerri, F. *Opt. Commun.* **1998**, *152*, 89.
(4) Zhang, G.; Wang, H.; Yu, Y.; Xiong, F.; Tang, G.; Chen, W. *Appl. Phys. B: Laser Opt.* **2003**, *76*, 677.
(5) Seo, J.; Kim, S.; Park, S. Y. *J. Am. Chem. Soc.* **2004**, *126*, 11154.
(6) Kim, S.; Seo, J.; Jung, H. K.; Kim, J. J.; Park, S. Y. *Adv. Mater.* **2005**, *17*, 2077.
(7) Lim, S. J.; Seo, J.; Park, S. Y. *J. Am. Chem. Soc.* **2006**, *128*, 14542.
(8) Seo, J.; Kim, S.; Lee, Y. S.; Kwon, O. H.; Park, K. H.; Choi, S. Y.; Chung, Y. K.; Jang, D. J.; Park, S. Y. *J. Photochem. Photobiol., A* **2007**, *191*, 51.
(9) Park, S.; Kim, S.; Seo, J.; Park, S. Y. *Macromol. Res.* **2008**, *16*, 385.
(10) Park, S.; Seo, J.; Kim, S. H.; Park, S. Y. *Adv. Funct. Mater.* **2008**, *18*, 726.
(11) Elsaesser, T.; Bakker, H. J. *Ultrafast Hydrogen Bonding Dynamics and Proton Transfer Processes in the Condensed Phase*; Kluwer Academic Publishers: Dordrecht, 2002.
(12) Douhal, A.; Kim, S. K.; Zewail, A. H. *Nature* **1995**, *378*, 260.
(13) Parasassi, T.; Krasnowska, E. K.; Bagatolli, L.; Gratton, E. *J. Fluoresc.* **1998**, *8*, 365.
(14) Kim, H. M.; Choo, H. J.; Jung, S. Y.; Ko, Y. G.; Park, W. H.; Jeon, S. J.; Kim, C. H.; Joo, T. H.; Cho, B. R. *ChemBioChem* **2007**, *8*, 553.
(15) Le Gourrierec, D.; Ormson, S. M.; Brown, R. G. *Prog. React. Kinet.* **1994**, *19*, 211.
(16) Abou-Zied, O. K.; Jimenez, R.; Thompson, E. H. Z.; Millar, D. P.; Romesberg, F. E. *J. Phys. Chem. A* **2002**, *106*, 3665.
(17) Zhong, D. P.; Douhal, A.; Zewail, A. H. *Proc. Natl. Acad. Sci. U.S.A.* **2000**, *97*, 14056.
(18) Nitzan, A. *Chemical Dynamics in Condensed Phases*; Oxford University Press: New York, 2006.
(19) Rhee, H.; Joo, T. *Opt. Lett.* **2005**, *30*, 96.
(20) Kim, C. H.; Joo, T. *Opt. Express* **2008**, *16*, 20742.
(21) Rhee, H.; Joo, T.; Aratani, N.; Osuka, A.; Cho, S.; Kim, D. *J. Chem. Phys.* **2006**, *125*, 074902.
(22) Manoj, P.; Min, C. K.; Aravindakumar, C. T.; Joo, T. *Chem. Phys.* **2008**, *352*, 333.
(23) Reichardt, C. *Solvents and Solvent Effects in Organic Chemistry*, 3rd ed.; Wiley-VCH: Weinheim, 2003.
(24) Woolfe, G. J.; Melzig, M.; Schneider, S.; Doerr, F. *Chem. Phys.* **1983**, *77*, 213.
(25) Wang, H.; Zhang, H.; Abou-Zied, O. K.; Yu, C.; Romesberg, F. E.; Glasbeek, M. *Chem. Phys. Lett.* **2003**, *367*, 599.
(26) Krishnamurthy, M.; Dogra, S. K. *J. Photochem.* **1986**, *32*, 235.
(27) Sobolewski, A. L.; Domcke, W. *Chem. Phys. Lett.* **1993**, *211*, 82.
(28) Sobolewski, A. L.; Domcke, W. *Chem. Phys.* **1994**, *184*, 115.
(29) Catalan, J.; Palomar, J.; dePaz, J. L. G. *J. Phys. Chem. A* **1997**, *101*, 7914.
(30) Scheiner, S. *J. Phys. Chem. A* **2000**, *104*, 5898.
(31) Hung, F. T.; Hu, W. P.; Chou, P. T. *J. Phys. Chem. A* **2001**, *105*, 10475.
(32) Aquino, A. J. A.; Lischka, H.; Hattig, C. *J. Phys. Chem. A* **2005**, *109*, 3201.
(33) Valeur, B. *Molecular Fluorescence*; Wiley-VCH: Weinheim, 2002.
(34) Jones, G.; Jackson, W. R.; Halpern, A. M. *Chem. Phys. Lett.* **1980**, *72*, 391.
(35) Turro, N. J. *Modern Molecular Photochemistry*; University Science Books: Sausalito, CA, 1991.
(36) Takeuchi, S.; Tahara, T. *J. Phys. Chem. A* **2005**, *109*, 10199.
(37) Kim, C. H.; Joo, T. *Phys. Chem. Chem. Phys.* **2009**, *11*, 10266.
(38) Kim, C. H.; Chang, D. W.; Kim, S.; Park, S. Y.; Joo, T. *Chem. Phys. Lett.* **2008**, *450*, 302.
(39) Chudoba, C.; Riedle, E.; Pfeiffer, M.; Elsaesser, T. *Chem. Phys. Lett.* **1996**, *263*, 622.
(40) Lochbrunner, S.; Wurzer, A. J.; Riedle, E. *J. Phys. Chem. A* **2003**, *107*, 10580.
(41) Lochbrunner, S.; Stock, K.; Riedle, E. *J. Mol. Struct.* **2004**, *700*, 13.
(42) Waluk, J. *Conformational Analysis of Molecules in Excited States*; Wiley-VCH: Weinhein, 2000.
(43) Shim, S.; Eom, I.; Joo, T.; Kim, E.; Kim, K. S. *J. Phys. Chem. A* **2007**, *111*, 8910.
(44) Douhal, A.; Fiebig, T.; Chachisvilis, M.; Zewail, A. H. *J. Phys. Chem. A* **1998**, *102*, 1657.
(45) Horng, M. L.; Gardecki, J. A.; Papazyan, A.; Maroncelli, M. *J. Phys. Chem.* **1995**, *99*, 17311.
(46) Middelhoek, E. R.; Zhang, H.; Verhoeven, J. W.; Glasbeek, M. *Chem. Phys. Lett.* **1997**, *267*, 525.
(47) Kang, T. J.; Jarzeba, W.; Barbara, P. F.; Fonseca, T. *Chem. Phys.* **1990**, *149*, 81.
(48) Simon, J. D.; Su, S.-G. *Chem. Phys.* **1991**, *152*, 143.

(49) Barbara, P. F.; Walker, G. C.; Smith, T. P. *Science* **1992**, *256*, 975.
(50) Tamai, N.; Nomoto, T.; Tanaka, F.; Hirata, Y.; Okada, T. *J. Phys. Chem. A* **2002**, *106*, 2164.
(51) Steinfeld, J. I.; Francisco, J. S.; Hase, W. L. *Chemical Kinetics and Dynamics*, 2nd Ed.; Prentice Hall: Upper Saddle River, NJ, 1999.
(52) Frisch, M. J.; Trucks, G. W.; Schlegel, H. B.; Scuseria, G. E.; Robb, M. A.; Cheeseman, J. R.; Montgomery, J. J. A.; Vreven, T.; Kudin, K. N.; Burant, J. C.; Millam, J. M.; Iyengar, S. S.; Tomasi, J.; Barone, V.; Mennucci, B.; Cossi, M.; Scalmani, G.; Rega, N.; Petersson, G. A.; Nakatsuji, H.; Hada, M.; Ehara, M.; Toyota, K.; Fukuda, R.; Hasegawa, J.; Ishida, M.; Nakajima, T.; Honda, Y.; Kitao, O.; Nakai, H.; Klene, M.; Li, X. K. J. E.; Hratchian, H. P.; Cross, J. B.; Bakken, V.; Adamo, C.; Jaramillo, J.; Gomperts, R.; Stratmann, R. E.; Yazyev, O.; Austin, A. J.; Cammi, R.; Pomelli, C.; Ochterski, J. W.; Ayala, P. Y.; Morokuma, K.; Voth, G. A.; Salvador, P.; Dannenberg, J. J.; Zakrzewski, V. G.; Dapprich, S.; Daniels, A. D.; Strain, M. C.; Farkas, O.; Malick, D. K.; Rabuck, A. D.; Raghavachari, K.; Foresman, J. B.; Ortiz, J. V.; Cui, Q.; Baboul, A. G.; Clifford, S.; Cioslowski, J.; Stefanov, B. B.; Liu, G.; Liashenko, A.; Piskorz, P.; Komaromi, I.; Martin, R. L.; Fox, D. J.; Keith, T.; Al-Laham, M. A.; Peng, C. Y.; Nanayakkara, A.; Challacombe, M.; Gill, P. M. W.; Johnson, B.; Chen, W.; Wong, M. W.; Gonzalez, C.; Pople, J. A.; Gaussian 03W, Revision D.0, Gaussian, Inc.: Wallingford CT, 2004.
(53) Chou, P. T.; Wu, G. R.; Wei, C. Y.; Shiao, M. Y.; Liu, Y. I. *J. Phys. Chem. A* **2000**, *104*, 8863.
(54) Okabe, C.; Nakabayashi, T.; Inokuchi, Y.; Nishi, N.; Sekiya, H. *J. Chem. Phys.* **2004**, *121*, 9436.
(55) Hsieh, C. C.; Cheng, Y. M.; Hsu, C. J.; Chen, K. Y.; Chou, P. T. *J. Phys. Chem. A* **2008**, *112*, 8323.
(56) Kosower, E. M.; Huppert, D. *Chem. Phys. Lett.* **1983**, *96*, 433.
(57) Sumi, H.; Marcus, R. A. *J. Chem. Phys.* **1986**, *84*, 4894.
(58) Cheng, Y. M.; Pu, S. C.; Yu, Y. C.; Chou, P. T.; Huang, C. H.; Chen, C. T.; Li, T. H.; Hu, W. P. *J. Phys. Chem. A* **2005**, *109*, 11696.
(59) Chou, P. T.; Martinez, M. L.; Clements, J. H. *J. Phys. Chem.* **1993**, *97*, 2618.
(60) Chou, P. T.; Pu, S. C.; Cheng, Y. M.; Yu, W. S.; Yu, Y. C.; Hung, F. T.; Hu, W. P. *J. Phys. Chem. A* **2005**, *109*, 3777.
(61) Cheng, Y. M.; Pu, S. C.; Hsu, C. J.; Lai, C. H.; Chou, P. T. *ChemPhysChem* **2006**, *7*, 1372.
(62) Roshal, A. D.; Organero, J. A.; Douhal, A. *Chem. Phys. Lett.* **2003**, *379*, 53.
(63) Shynkar, V. V.; Mely, Y.; Duportail, G.; Piemont, E.; Klymchenko, A. S.; Demchenko, A. P. *J. Phys. Chem. A* **2003**, *107*, 9522.

JP909438P